Eur. Phys. J. E **21**, 161–174 (2006)
DOI 10.1140/epje/i2006-10057-5

THE EUROPEAN PHYSICAL JOURNAL E

Dewetting of thin polymer films

T. Vilmin[a] and E. Raphaël

Laboratoire de Physico-Chimie Théorique, UMR CNRS 7083, ESPCI, 10 rue Vauquelin, 75231 Paris Cedex 05, France

Received 4 July 2006 and Received in final form 31 October 2006 /
Published online: 5 December 2006 –

Abstract. We study the dewetting of thin polymer films deposited on slippery substrate. Recent experiments on these systems have revealed many unexpected features. We develop here a model that takes into account the rheological properties of polymer melts, focussing on two dewetting geometries (the receding of a straight edge, and the opening of a hole). We show that the friction law associated with the slippage between the film and the substrate has a direct influence on the dewetting dynamic. In addition, we demonstrate that residual stresses, which can be stored in the films due to their viscoelasticity, are a source of destabilization for polymer films, and accelerate the dewetting process.

PACS. 68.60.-p Physical properties of thin films, nonelectronic – 68.15.+e Liquid thin films – 68.55.-a Thin film structure and morphology – 83.10.-y Fundamentals and theoretical

1 Introduction

If the spreading parameter $S = \gamma_{sv} - \gamma_{sl} - \gamma$ is negative, a liquid film deposited onto a flat substrate is thermodynamically unstable when thinner than the critical thickness $(2\gamma/\rho g)^{1/2} \sin(\theta/2)$ (γ_{sv}, γ_{sl}, and γ are, respectively, the solid-vapor, solid-liquid, and liquid-vapor surface energy, and θ is the Young contact angle $\cos\theta = 1 + S/\gamma$; ρ is the density of the liquid, and g is the gravity acceleration. [1]). It means that holes will appear in the film, and dry patches will grow until only isolated droplets remain onto the substrate: the film dewets. The dynamic of the flows that appear during the dewetting of liquid films is controlled by the different existing sources of dissipation.

The peculiarity of polymer films is that the entanglements between the chains allow the lower chains to slip onto the substrate if this one is smooth and passive. One commonly characterizes the slippage by the hydrodynamic extrapolation length (or slip length) $b = \eta/\zeta$ [1], where η is the viscosity of the liquid, and ζ is the friction coefficient related to a linear interfacial force (per unit surface) of the liquid on the substrate $f = \zeta v_{slip}$. The theoretical prediction for the length b in the steady-state flow of a polymer melt is $a(N^3/P^2)$, where a is the monomer size, N is the polymerization index, and P the entanglement index of the polymer liquid [2]. If the substrate is itself a liquid layer of thickness $e > a$ and viscosity η', b is even increased: $e(\eta/\eta')$. Now, if the slip length b is larger than the thickness h_0 of the polymer film, the vertical velocity gradients are small compared with the horizontal ones, and the dewetting of the film can be roughly described as a plug flow. The dissipation sources are then the horizontal velocity gradients, and the slippage at the liquid-substrate interface. For high-molecular-weight polymers, the viscosity is large ($\eta \gg \sqrt{\rho|S|b}$) and inertial effects can be omitted.

Some years ago, Brochard-Wyart *et al.* [3,4] (hereafter cited as BW) initiated the experimental and theoretical study of the dewetting of thin films, assuming the film thickness to be smaller than the slip length b (high-slip regime). Comparing the dissipation due to interfacial friction with the viscous dissipations in the radial flow associated to the opening of a hole in a flat film, BW introduced the characteristic length $\Delta = \sqrt{h_0 b} = \sqrt{h_0\eta/\zeta}$. Then, BW described the opening of a hole in three steps: As long as the hole radius R is smaller than Δ, the viscous dissipations due to radial and orthoradial deformations dominate over the dissipation due to interfacial friction, leading to an exponential growth of the hole. When $R > \Delta$, the friction dominates over the viscous dissipation, and the radial geometry (hole geometry) does not play any role any more. The problem can then be reduced to the two-dimensional problem of a film dewetting from a straight edge (edge geometry). In this geometry, two time regimes appear: In the first regime, a rim of width Δ builds up and the dewetting velocity is constant in time. In the second regime, after the dewetted distance R has reached a value of order b, the rim becomes "mature", that is rounded by the surface tension, and the velocity decreases proportionally to $t^{-\frac{1}{3}}$.

During the "mature-rim" regime, the morphology of the rim is fixed by the surface tension and the dynamic depends only weakly on the film rheology. On the other hand, when the rim builds up (first regime), the surface

[a] e-mail: thomas.vilmin@gmail.com

tension is only effective on a small part of the rim, thus allowing unusual morphologies and dynamics. The energetic approach used by BW, though very powerful to establish scaling laws, is unable to handle the description of the building rim morphology. Moreover, they limited the use of this method to Newtonian liquids. Though, if polymer entanglements lead to slippage, they also bring about non-Newtonian rheologies such as viscoelasticity [5]. Additionally, as the substrates are always coated in order to be flat and passive, the friction force rarely varies linearly with the slip velocity, which means that the slip length is not constant [6,7].

Ever since this early important work of BW, enormous efforts have been developed towards the study of the dewetting of thin polymer films [8–26]. A special attention has been paid to the birth of the rim (note that rims have only been observed for polymer films [18–26]). Systematic studies on thin polystyrene (PS) films deposited on highly slippery substrates have set the principal features associated with the building up of the rim in the edge geometry [22,23,25,26]. A rapid decrease of the dewetting velocity, as t^{-1}, starting from unexpectedly high initial velocities of the order of $1\,\mu\mathrm{m\,s^{-1}}$ is observed. This is associated to the building of a very asymmetric rim, with an extremely steep side towards the bare substrate and a much slower decay on the rear side. The rim width increases logarithmically with time, proportionally to the dewetted distance. After a certain characteristic time, the rim width reaches a maximum and then slowly decreases, while the dewetting velocity begins to level off. Important variations of the initial dewetting velocity, and of the maximum rim width, with the age of the samples conserved below T_g have been noticed. It happens that the initial dewetting velocity and the maximum rim width decrease when increasing the conservation time. This feature has been attributed to the presence of residual stresses which could result from the spin coating process. Indeed, this process leads to a fast evaporation of the solvent, and lets the polymer molecules in a non-equilibrium frozen-in state [24–27]. Such residual stresses have recently been clearly revealed experimentally by Bodiguel and Fretigny [28].

In this paper, we first focus on the straight-edge dewetting geometry. This is motivated by the following reasons: firstly, the flow is simpler than in the hole geometry, and, secondly, BW has shown that for a large enough radius the dynamic of hole opening becomes similar to the dynamic in the straight-edge geometry. Additionally, the fact that the surface tension is ineffective allows us to study the direct influence of the friction and of the film rheology. We propose a mechanical study, composed of an analytical part and a numerical part, which explains the asymmetric morphology of the rim. We then use BW energetic analysis to study the dynamic of the dewetting of viscoelastic liquid films. We also take residual stresses into account, as well as the possibility of a non-linear dependence of the friction force on the slip velocity. A rather general description of the dynamic of the birth of the rim is then developed, allowing a quantitative evaluation of the residual stresses, and a characterization of the film rheology and of the friction between the film and the substrate.

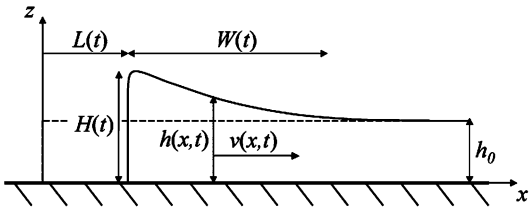

Fig. 1. Film geometry: $h(x,t)$ is the profile of the film, h_0 is the initial height of the film, $H(t)$ is the height of the front, $L(t)$ is the dewetted distance, $W(t)$ is the width of the rim, and $v(x,t)$ is the horizontal velocity of the film.

In the last part of the paper (Sect. 6), we address the dewetting process in the hole geometry, which is very commonly studied experimentally [16–23]. Though the flow is slightly more complicated then, the fact that the role of the friction is reduced during the first stage of the opening of a hole, as shown by BW, allows for a rather simple description of the phenomenon. We then study the consequences of the viscoelastic and residual stresses on the dewetting dynamic in this hole geometry.

2 Mechanical study for Newtonian liquids

2.1 Analytical mechanical analysis

Aiming at the description of the building up of the rim, we consider the dewetting of a liquid film from a straight edge (reducing the study to a two-dimension problem in the xOz-plane), neglecting inertia and the film surface tension. We describe the velocity field using its horizontal component v and its vertical component w. The film is initially flat, with a vertical front at the position $x = 0$, and is infinitely spreading in the $x > 0$ half-space. We assume that the thickness of the liquid film $h(x,t)$ is much smaller than the hydrodynamic extrapolation length $b = \eta/\zeta$. Then, the vertical variations of the horizontal velocity $\partial_z v \sim v/b$ are very small, and we can consider that the horizontal velocity $v(x,t)$ does not depend on the vertical coordinate z (see Fig. 1). In this plug-flow regime, volume conservation $\partial_x v + \partial_z w = 0$ leads to strain rates $\partial_x v$ and $\partial_z w$ that do not depend on z. Then, the horizontal normal stresses $\sigma = \eta\partial_x v - P$ (where P is the pressure within the film) does not depend on z either, since the Navier-Stokes equation projected along the Oz-direction reads $\eta\partial_{zz} w - \partial_z P = 0$. We neglect the Laplace pressure (for it has only an influence on a very small part of the rim, this point will be discussed in Sect. 2.4), as well as the vapor pressure. This implies that the film-air interface is stress free and that the vertical normal stress is nil (in the $\partial_x h \ll 1$ limit that applies if $h_0 \ll b$). This leads to the inner pressure $P(x,t) = \eta\partial_z w = -\eta\partial_x v$, and to the horizontal normal stresses $\sigma(x,t) = 2\eta\partial_x v$. Considering the friction force $-\zeta v(x,t)$ per unit surface on the substrate, and since no exterior forces act on the surface

of the film, the horizontal momentum equation integrated over the thickness of the film reads

$$\zeta v = \frac{\partial\left(h\sigma\right)}{\partial x} = 2\eta\frac{\partial}{\partial x}\left(h\frac{\partial v}{\partial x}\right). \tag{1}$$

This equation comes with two boundary conditions at the edges of the film. The applied force per unit of length, $|S|$, pushing the film away from the dry area, fixes the viscous stress at the edge:

$$\frac{|S|}{H} = -\sigma(L), \tag{2}$$

where $H = H(t)$ is the front height, and $L = L(t)$ is the dewetted distance (see Fig. 1). At the opposite of the film, infinitely far away in the $x > 0$ direction, the velocity must vanish and the film stays unperturbed. In addition, assuming the fluid to be incompressible, the volume conservation leads to the relation

$$\frac{Dh}{Dt} = \frac{\partial h}{\partial t} + v\frac{\partial h}{\partial x} = -h\frac{\partial v}{\partial x}. \tag{3}$$

The above equations can be solved at short times, when $h(x,t)$ is very close to h_0. The velocity field is then simply given by

$$v(x,t) = V\exp\left(-\frac{x-L}{\sqrt{2}\Delta}\right), \tag{4}$$

where the length

$$\Delta = \sqrt{h_0 b} = \sqrt{\frac{h_0\eta}{\zeta}} \tag{5}$$

is the one defined by BW, and the velocity

$$V = \frac{|S|}{\sqrt{2\zeta\eta h_0}} = \frac{\Delta}{\sqrt{2}\tau} \tag{6}$$

deduced from equation (2), with $\tau = h_0\eta/|S|$, is the dewetting velocity found by the same authors [4]. Note that the lubrication approximation is not valid here since the second derivative along the vertical direction $\partial_{zz}v \sim V/b^2$ is very small compared to the horizontal one $\partial_{xx}v \sim V/\Delta^2 = V/(hb)$. Additionally to the evaluation of the dewetting velocity already made by BW, the present mechanical analysis provides information about the film morphology. Indeed, the evolution of the front height is given by equations (2) and (3):

$$H(t) = h_0\left(1 + \frac{t}{2\tau}\right). \tag{7}$$

Since the velocity field decreases exponentially as one moves away from the front, the film profile exhibits, at short times, an asymmetric rim, with an exponential decrease of the height over the characteristic length Δ:

$$h(x,t) = h_0\left(1 + \frac{t}{2\tau}\exp\left(-\frac{x-L}{\sqrt{2}\Delta}\right)\right). \tag{8}$$

This shape is indeed the one observed by Reiter on AFM images [19]. In the absence of surface tension, the damping of the film velocity by the friction over the length Δ is responsible for the rising of the asymmetric rim. However, the present resolution of the equations of the flow only holds for times shorter than τ, and does not allow to determine the time evolution of the dewetting velocity V. In the next section we review the energetic approach used by BW. It reveals itself as the best way to establish the scaling laws which characterize the dewetting of simple and complex liquid films, completing the mechanical approach.

2.2 Energy balance

The dewetting velocity V for a Newtonian thin film has already been evaluated by BW [4] using simple energetic arguments. In this subsection we reconsider this problem using the mechanical study developed above. The energy balance imposes that the viscous dissipations within the film $T\dot{S}_{visc}$, and the dissipation due to the friction at the interface with the substrate $T\dot{S}_{fric}$, match the work $|S|V$ done by the capillary forces per unit of time. The viscous dissipation is related to the normal stresses in the horizontal and vertical direction, and also to the shear stress. One can compare the order of magnitude $\eta\partial_z v \sim \eta V/b$ of the latter to the one of the normal stresses $\eta\partial_x v \sim \eta V/\Delta$, and show that it is negligible. Then, using the velocity field (4), one gets the viscous dissipation

$$T\dot{S}_{visc} = \eta\int_L^\infty 2h\left(\frac{\partial v}{\partial x}\right)^2 \mathrm{d}x = \frac{1}{\sqrt{2}}\zeta\Delta V^2 \tag{9}$$

and the dissipation due to friction reads

$$T\dot{S}_{surf} = \zeta\int_L^\infty v^2\mathrm{d}x = \frac{1}{\sqrt{2}}\zeta\Delta V^2. \tag{10}$$

As expected, the equality $|S|V = T\dot{S}_{visc} + T\dot{S}_{fric}$ gives the expression $V = |S|/(\sqrt{2}\zeta\Delta) = \Delta/\sqrt{2}\tau$ of the initial dewetting velocity. We notice that, contrary to what BW conjectured, the viscous dissipation is not negligible but equal to the dissipation due to friction. Nevertheless, the scaling of V remains unchanged whether $T\dot{S}_{visc} = T\dot{S}_{fric}$ or $T\dot{S}_{visc} \ll T\dot{S}_{fric}$.

The time evolution of the dewetting velocity can now be determined from simple scaling arguments: the interfacial dissipation is approximately $T\dot{S}_{surf} \simeq \zeta WV^2$, while from (1) we deduce the scaling $(\partial_x v)^2 \sim \zeta v^2/\eta h$, and the viscous dissipation reads $T\dot{S}_{visc} \simeq \zeta WV^2$, where W is the rim width. This width is given by the volume conservation and equation (7): $W(t) \simeq h_0 L(t)/(H(t) - h_0) = L(t)2\tau/t$. Therefore, the interfacial and viscous dissipations stay of the same order and almost constant, even for larger times than τ. Moreover, the dewetting velocity and the rim width remain also approximately constant, as BW predicted it.

In what follows we will mostly be interested in establishing scaling laws concerning the dewetting of complex fluids, whose dynamics cannot be solved exactly. We will

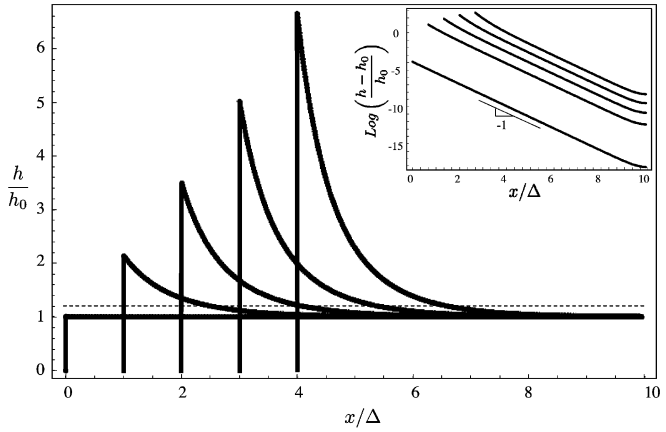

Fig. 2. Numerical calculation of the shape of a Newtonian film dewetting on a slippery substrate at different times. The different curves are separated by the same time interval Δ/V_0. The inset shows the logarithm of $(h-h_0)/h_0$ at the same times.

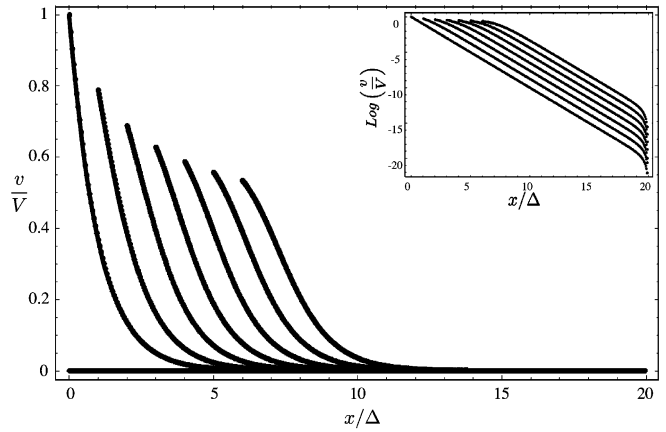

Fig. 3. Numerical calculation of the horizontal velocity in a Newtonian film dewetting on a slippery substrate at different times. The different curves are separated by the same time interval Δ/V_0. The inset shows the logarithm of v/V at the same times.

thus systematically use the assumption $T\dot{S}_{visc} \lesssim T\dot{S}_{fric}$, and write the simplified energy balance $|S|V \simeq \zeta W V^2$. Then, the dewetting velocity V can be deduced from the evolution of the rim width $W \simeq Lh_0/(H-h_0)$. Finally, the scaling laws describing the whole dewetting dynamic can be deduced from the evaluation of $H(t)$:

$$|S|V \simeq \zeta \frac{h_0}{H-h_0} LV^2 \qquad (11)$$

for any kind of liquid, as long as the slip length b is large compared with the film thickness. Since this analytical method gives approximated results, it is of interest to compare them with results obtained numerically.

2.3 Numerical calculations

We numerically integrated the equations of the flow (1) and (3) along with the boundary condition (2) and a

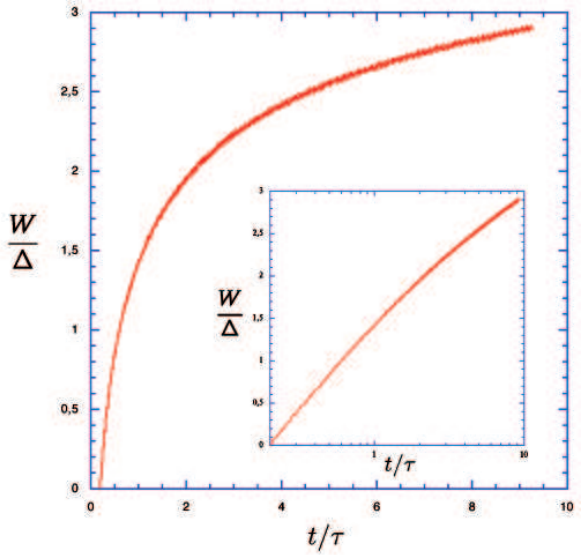

Fig. 4. Numerical calculation of the reduced dewetting rim width W/Δ *versus* the reduced time t/τ for a Newtonian film. A linear-log plot is shown in the inset.

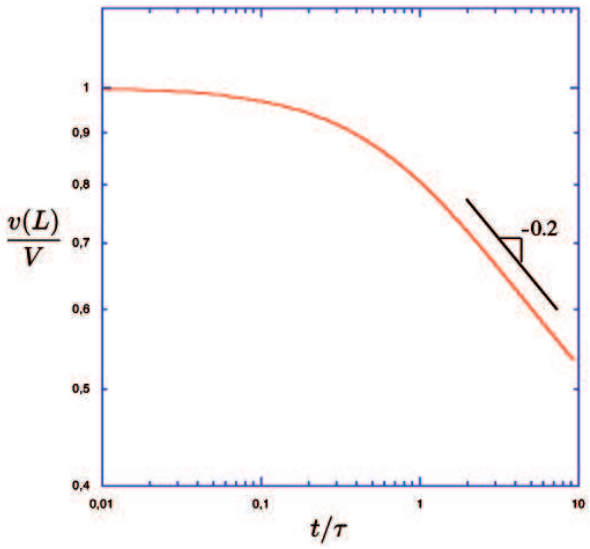

Fig. 5. Numerical calculation of the reduced dewetting velocity $v(L)/V$ *versus* the reduced time t/τ for a Newtonian film. The straight line represents $t^{-0.2}$.

shooting procedure from the velocity $V(t) = v(L,t) = \dot{L}(t)$ at the edge of the film, toward the target $v = 0$ far in the Ox-direction, where the film should remain unperturbed. We consider finite-size films (much larger than Δ) with a vertical front at the position $x = L$. This numerical method gives the fields $h(x,t)$ and $v(x,t)$ in the whole film (see Figs. 2 and 3), from which we deduce $H(t)$, $L(t)$, $V(t)$ and $W(t)$ (see Figs. 4 and 5). The width of the rim W is defined as the distance between the edge and the position where the thickness $h(x,t)$ is 1/5 larger than the initial thickness h_0. It is of the same order as Δ (from Eq. (8) we deduce that $W = \sqrt{2}\Delta \ln(5t/\tau)$). This numerical work confirmed that both the velocity and the rim

height decrease exponentially over the constant distance Δ, even after several times τ and $H(t) \gg h_0$. It also confirmed that the dewetting velocity stays approximately constant (a slow decrease $\sim t^{-0.2}$ is noticed). The exact analytical result of a linear increase of the rim height $H(t)$ is verified. The very good agreement between the analytical mechanic and energetic approaches, and the numerical method attests to the validity of the approximations made in the analytical developments, as well as it attests to the validity of the numerical results.

However, a constant dewetting velocity is not observed experimentally, but rather a rapid decrease of the velocity, proportionally to $1/t$. We expect this discrepancy to come from the non-Newtonian behavior of the polystyrene films used in these experiments, and in particular from their viscoelastic behavior (see Sect. 3).

If the system composed of equations (1) and (3) is impossible to solve analytically for complex liquids, it can be solved numerically for any kind of liquid. Hence, this numerical code will be a very useful tool to study complex liquids, and verify the predictions which can be made by approximated analytical analysis. Before we address the case of viscoelastic films, we will evaluate the effects of the surface tension that has been neglected from the beginning of this study.

2.4 Consequences of surface tension

The surface tension, of course, is always present, it has just negligible effects during this first part of the rim growth. Its principal consequence is to round the rim so that it forms the Young angle θ with the substrate at equilibrium ($-S \simeq \theta^2\gamma/2$ for small angles). The edge of the rim is then cylindrical over the width $2h_0/\theta$. The equilibrium is roughly reached around the time $\theta h_0/|S|$, which is small compared to the time $\tau = \eta h_0/|S|$ for small angles. Therefore, one can consider that the rim presents a cylindrical pre-section at the front, whose width is $\delta \simeq H/\theta$. The rim remains highly asymmetric if $\delta \ll \Delta$, that is to say as long as $H(t) \ll \theta\Delta$. Hence, if $h_0 > \theta\Delta$, *i.e.* $\theta < \sqrt{h_0/b}$, the asymmetric-rim regime does not exist. On the other hand, if $\theta \gg \sqrt{h_0/b}$, the rim is highly asymmetric as long as $L(t) \ll \theta b$. Given the constant dewetting velocity V, the asymmetric-rim regime lasts until the time $\theta b/V = \theta\sqrt{b/h_0}(h_0\eta/|S|)$. When $L \geq \theta b$, the friction of the cylindrical section on the substrate is more important than the friction of the rest of the film. Note that simultaneously the Laplace pressure due to the curvature of the exponentially decaying rim becomes of the same order as the capillary pressure $|S|/H$, which is the Laplace pressure within the cylindrical section. Thus, once $L \geq \theta b$, the "mature-rim" regime, first described by BW, begins: the rim shape is round and symmetric as fixed by the surface tension, whose width $W \sim \sqrt{h_0 L/\theta}$ is simply given by volume conservation. The energetic approach can be applied in the "mature-rim" regime: the viscous dissipation is still approximately given by the expression $T\dot{S}_{visc} \sim \zeta\Delta V^2$, while the interfacial dissipation $T\dot{S}_{surf} \sim \zeta W V^2$ is much larger. Then, the energy balance reads $|S|V \simeq \zeta\sqrt{h_0 L/\theta}V^2$, which gives a $t^{-\frac{1}{3}}$ decrease of the velocity [3, 4,12–15,18]. Note that the rheologic properties of the liquid do not play any role in this regime, as the morphology of the rim is imposed by the surface tension. The following study will be only focussed on the building of the asymmetric rim during which the surface tension is negligible, assuming $h_0 < \theta^2 b$. This condition is well respected in [22, 23,25,26], where $\theta \simeq 0.5$ rad and b/h_0 is larger than 10^4.

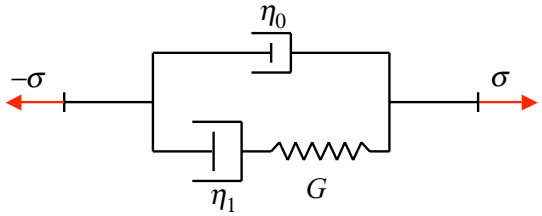

Fig. 6. Rheologic model of a Jeffreys viscoelastic liquid.

3 Viscoelastic films

3.1 Constitutive rheologic equation

One of the most important properties of polymer molecules is that they can entangle one with each other. These entanglements between chains give to polymer melts a transient elasticity, which is call viscoelasticity. In the simplest cases it can be characterized by an elastic modulus G and a relaxation time τ_1 (in the bulk, τ_1 would be the reptation time of the polymer chains, but it may be different in thin films), accounting for an elastic solid behavior at times shorter than τ_1, and for a Newtonian behavior, with the high viscosity $\eta_1 = \tau_1 G$, at longer times. At very short times ($t \ll \tau_0 \ll \tau_1$) the rheology is in fact dominated by the friction between monomers, giving a low-viscosity Newtonian response, with $\eta_0 = \tau_0 G \ll \eta_1$. η_0 and η_1 are the elongational viscosities of the melt. With the three parameters G, η_0 and η_1 we can set the relatively simple constitutive equation, which corresponds to an improved Maxwell's model called Jeffreys' model [5,15,24] (see Fig. 6):

$$G\sigma + \eta_1\dot{\sigma} = G\eta_1\dot{\gamma} + \eta_0\eta_1\ddot{\gamma}, \tag{12}$$

where $\dot{\gamma} = \partial_x v$ is the strain rate, and $\ddot{\gamma}$ is its time derivative. This linear constitutive equation can be rewritten for the Fourier transforms $\tilde{\sigma}(\omega)$ and $\tilde{\gamma}(\omega)$. Note that using the equivalence between the inverse of the frequency $1/\omega$ and the time t [29], one can define an effective viscosity $\eta_{eff} = Gt$ during the elastic regime ($\tau_0 \ll t \ll \tau_1$). This regime is of great importance when the time τ_1 is large. If close to the glass transition, this time can easily be much longer than a day. It is impossible, in these cases, to neglect viscoelasticity in the study of the dewetting. Note that the time τ_0 is typically too short for the first Newtonian regime to be observed in dewetting experiments.

3.2 Consequences on dewetting

Since τ_0 is much smaller than τ_1, the three characteristic behaviors corresponding to the three regimes are very well separated: short-times Newtonian response (η_0, $t \ll \tau_0$), intermediate-times elastic response (G, $\tau_0 \ll t \ll \tau_1$), and long-times Newtonian response (η_1, $\tau_1 \ll t$). Consequently, they can be schematically transposed to the dewetting dynamic:

- For times shorter than τ_0, the viscoelastic liquid dewets like a simple liquid, with the high constant velocity $V_0 = |S|/\sqrt{2\zeta\eta_0 h_0}$, and with the birth of an asymmetric rim of width $\Delta_0 = \sqrt{h_0\eta_0/\zeta}$.
- At long times ($t > \tau_1$), the viscoelastic liquid also dewets like a simple liquid, but with the constant velocity $V_1 = |S|/\sqrt{2\zeta\eta_1 h_0} = V_0\sqrt{\eta_0/\eta_1} \ll V_0$, and with the formation of an asymmetric rim of width $\Delta_1 = \sqrt{h_0\eta_1/\zeta} = \Delta_0\sqrt{\eta_1/\eta_0} \gg \Delta_0$.
- In between these two regimes, the elastic behavior of the fluid will thus lead to a significant drop of the dewetting velocity. We can study the dewetting dynamic using the energy balance equation (11), assuming that the viscous dissipation and the time variation of the elastic energy are smaller than or equal to the interfacial dissipation. Then, we only need to evaluate the height $H(t)$ of the rim, which is given by equations (2, 3) and (12):

$$\frac{|S|}{H} + \tau_1 \frac{\mathrm{d}}{\mathrm{d}t}\left(\frac{|S|}{H}\right) = \tau_1 G\left(\frac{\dot{H}}{H} + \tau_0 \frac{\mathrm{d}}{\mathrm{d}t}\left(\frac{\dot{H}}{H}\right)\right). \quad (13)$$

At short times $H(t)$ increases at the constant rate $|S|/\eta_0$, since the rheology is Newtonian-like. Around τ_0 the polymer chains are stretched, and the elasticity prevents the height of the rim $H(t)$ from increasing more at the same rate. Then, only the disentanglement allows $H(t)$ to increase at the rate $|S|/2\eta_1$. Therefore, between τ_0 and τ_1 the height of the rim only weakly increases above $H_0 \simeq h_0 + |S|/G$ (assuming $|S| < h_0 G$, more generally, H_0 is defined by $(H_0/h_0)\ln(H_0/h_0) = |S|/(h_0 G)$). Hence, we can consider $H(t)$ as a constant, which imposes the width of the rim $W(t)$ to increase proportionally to the dewetted distance $L(t)$:

$$W \simeq \frac{G}{|S|} h_0 L. \quad (14)$$

Then, equation (11) gives

$$V(t) \simeq \frac{|S|}{\sqrt{2\zeta G h_0 t}} = V_1 \left(\frac{t}{\tau_1}\right)^{-1/2}. \quad (15)$$

As in the "mature-rim" regime, it is the increase of the rim width which is responsible for the slowing-down of the dewetting during the elastic regime. The rim width increasing rate is here maximum, for its height is constant in time. In this friction-driven dynamic, this maximum increasing rate of the rim width leads to the most rapid velocity decrease. Indeed, no other rheological model, whether it uses viscoelasticity or shear thinning, can lead to a more rapid decrease of the velocity than $t^{-1/2}$, if the friction dominates and linearly depends on the slip velocity. Interestingly, we remark that a purely elastic film would dewet at a velocity scaling like $t^{-1/2}$ over an infinite distance, since the strong slippage allow the deformation to remain finite.

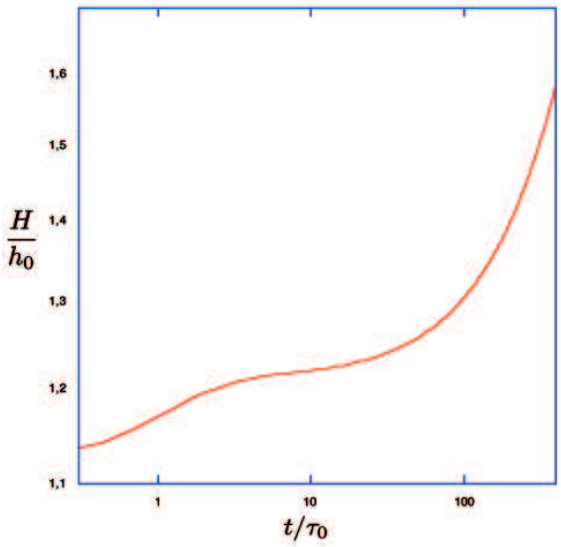

Fig. 7. Numerical calculation of the reduced rim height H/h_0 *versus* the reduced time t/τ_0 for a viscoelastic film with $\tau_1 = 100\,\tau_0$, and $h_0 G/|S| = 10$.

Note that we could have simply deduced the scaling law $V(t) \simeq V_1\sqrt{\tau_1/t} = V_0\sqrt{\tau_0/t}$ from the relation $V_1/V_0 = \sqrt{\tau_0/\tau_1}$. Or else, we could have used the effective viscosity $\eta_{eff} = Gt$ in expression (6) of the dewetting velocity, which simply gives the scaling $V(t) \simeq V_0\sqrt{\tau_0/t}$ [30].

We confirmed these analytical predictions by the resolution of the equations of the flow with the numerical method proposed above (see Figs. 7 and 8). The perfect agreement between our analytical and numerical results indicates that our assumption that the bulk viscous dissipation and the elastic-energy variation are smaller than or equal to interfacial dissipation does hold for the viscoelastic liquid described by equation (12). In fact, a straightforward evaluation of the stored elastic energy would show that its time derivative is equal to the interfacial dissipation.

As for a Newtonian liquid, the building up of the rim precedes the "mature-rim" regime. The characteristic time which marks the transition between these two regimes is $\theta b_1/V_1 = \theta\sqrt{b/h_0}(2h_0 G/|S|)\tau_1 > \tau_1$, where $b_1 = \eta_1/\zeta$ is the steady-state slip length.

According to our model, the viscoelasticity of polymer films explains two characteristic features of the dewetting of PS films [22,23]:
a) The proportionality between the dewetted distance and the width of the rim is a consequence of the entanglements, which prevent the height of the rim to increase between τ_0 and τ_1.

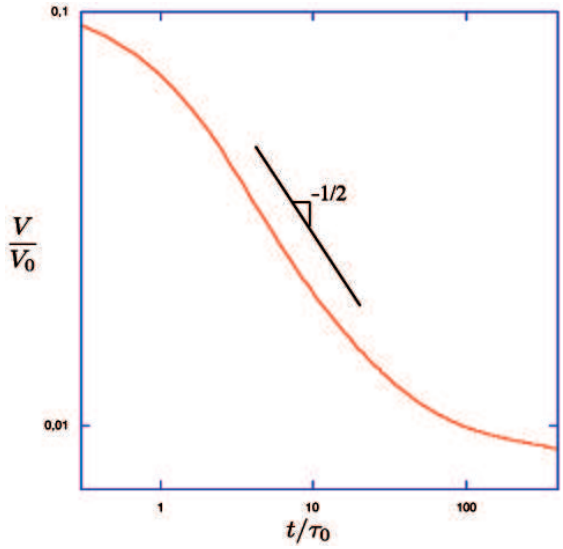

Fig. 8. Numerical calculation of the reduced dewetting velocity V/V_0 *versus* the reduced time t/τ_0 for a viscoelastic film with $\tau_1 = 100\,\tau_0$, and $h_0 G/|S| = 10$. The straight line represents $t^{-\frac{1}{2}}$.

b) The very high initial dewetting velocity results from the fact that the entanglements are unaffected at short times ($t < \tau_0$), giving a ratio $V_0/V_1 = \sqrt{\tau_1/\tau_0} \gg 1$.

On the other hand, the predicted decreasing law of the velocity ($V \sim t^{-1/2}$) is slower than what is observed ($V \sim t^{-1}$). We will see in the forthcoming section that the power law of the velocity decrease is dependent on the type of friction being effective between the film and the substrate, and that in some situations the decrease of the velocity can be greatly accelerated.

4 Non-linear friction

4.1 Origins and first consequences

Up to now, we have assumed the simplest possible form for the friction law, that is a linear dependence of the friction force on the velocity. The friction has not in fact any strong reason to be so, especially because the substrates are very often coated with a polymer layer in order to be smooth and passive. For example, in many experiments where PS film are used, the substrate is a silicon wafer coated with a polydimethylsiloxane (PDMS) mono-layer [18,19,22,23,25]. Several friction experiments have been done on grafted or absorbed PDMS surfaces, which have shown a very weak increase of the friction force with velocity: Casoli *et al.* measured a friction force increasing proportionally to $V^{\frac{1}{3}}$ between a PDMS elastomer and an absorbed brush, and only like $V^{\frac{1}{6}}$ on dense grafted brushes, for sliding velocities between $10\,\mu\mathrm{m\,s^{-1}}$ and $5\,\mathrm{mm\,s^{-1}}$ [6]. More recently Bureau *et al.* showed a $V^{\frac{1}{5}}$-dependence of the friction force between an elastomer and a grafted brush, for sliding velocities ranging from $300\,\mu\mathrm{m\,s^{-1}}$ down to $0.01\,\mu\mathrm{m\,s^{-1}}$ [7], which is the velocity range of the dewetting experiments. These results are reminiscent of a solid friction independent of the sliding velocity.

A rather general expression of the friction force by surface unit is

$$f_r = \begin{cases} \zeta v, & \text{for} \quad v < v_\alpha\,, \\ \zeta v_\alpha \left(\frac{v}{v_\alpha}\right)^{1-\alpha}, & \text{for} \quad v > v_\alpha\,, \end{cases} \tag{16}$$

where α is a shear-thinning exponent smaller than unity ($\alpha = 0$ would correspond to the case of linear friction). According to the reported friction experiments, α could range between 2/3 and 5/6. The effective friction coefficient is then a decreasing function of v (as well as the inverse of the slip length): $\zeta_{eff}(v) = \zeta(v_\alpha/v)^\alpha$, where v_α is the velocity below which the friction coefficient remains equal to ζ correspondingly to a linear friction. This linear regime can be omitted if the dewetting velocity is much larger than v_α (when the velocity in most of the rim is larger than v_α). Hereafter, we assume this condition to hold during the whole dewetting process, even if it may not be the case at the end of the dewetting experiments. The increase of the effective friction coefficient when decreasing the sliding velocity lets us expect an intensified decrease of the dewetting velocity for viscoelastic films. More tentatively, the $\zeta^{-\frac{1}{2}}$-dependence of the rim width Δ could bring about a decrease of the rim width associated with the decrease of the dewetting velocity, as observed experimentally.

Considering such a friction force and a Newtonian fluid of viscosity η, the momentum equation (1) becomes

$$\zeta v_\alpha \left(\frac{v}{v_\alpha}\right)^{1-\alpha} = 2\eta \frac{\partial}{\partial x}\left(h \frac{\partial v}{\partial x}\right). \tag{17}$$

This latter relation replace equation (1) in the system composed of equations (1) to (3) characterizing the dewetting flow. As long as h remains of the order of h_0, the solution is given by

$$v(x,t) = V_\alpha \left(1 - \frac{\alpha}{2}\frac{x-L}{\sqrt{2}\Delta_\alpha}\right)^{\frac{2}{\alpha}} \tag{18}$$

when $x - L < \Delta_\alpha$, and $v(x,t) = 0$ elsewhere. Here, the dewetting velocity

$$V_\alpha = \left(\left(\frac{2-\alpha}{2}\right)\frac{V^2}{v_\alpha^\alpha}\right)^{\frac{1}{2-\alpha}} \simeq \frac{|S|^{\frac{2}{2-\alpha}}}{(\zeta\eta h_0)^{\frac{1}{2-\alpha}} v_\alpha^{\frac{\alpha}{2-\alpha}}} \tag{19}$$

is constant in time, as well as the rim width

$$\Delta_\alpha = \left(\left(\frac{2-\alpha}{2}\right)\frac{V^\alpha}{v_\alpha^\alpha}\right)^{\frac{1}{2-\alpha}} \Delta \simeq \left(\frac{|S|}{\zeta v_\alpha}\right)^{\frac{\alpha}{2-\alpha}} \left(\frac{h_0\eta}{\zeta}\right)^{\frac{1-\alpha}{2-\alpha}} \tag{20}$$

(V and Δ are defined by Eqs. (5) and (6)). These analytical results are once again confirmed by the numerical results.

As the importance of the viscoelasticity in the dewetting has been demonstrated, we will now study the combined effects of non-linear friction and viscoelasticity.

4.2 Viscoelastic liquids

The study of the dewetting of a viscoelastic film in the presence of non-linear friction is similar to the one we developed in the previous section with a linear-friction force. The three time regimes will structure the dewetting process in the same way: the short times and long times will bring Newtonian-like dewetting, whereas the intermediate times will be the place of an elastic response. Only the dissipation due to the friction is modified, and equation (11) is replaced by the energy balance equation:

$$|S|V \simeq \zeta v_\alpha \frac{h_0}{H-h_0} LV \left(\frac{V}{v_\alpha}\right)^{1-\alpha}, \qquad (21)$$

where the time evolution of $H(t)$ does not depend on the friction law.

- Therefore, the viscoelastic film we described earlier starts dewetting with the velocity $V_{0\alpha} = ((\frac{2-\alpha}{2})V_0^2/v_\alpha^\alpha)^{\frac{1}{2-\alpha}}$, building up a rim of characteristic width $\Delta_{0\alpha} = ((\frac{2-\alpha}{2})V_0^\alpha/v_\alpha^\alpha)^{\frac{1}{2-\alpha}}\Delta_0$ until the time τ_0.
- After the time τ_1 the dewetting is much slower, stabilized at the velocity $V_{1\alpha} = ((\frac{2-\alpha}{2})V_1^2/v_\alpha^\alpha)^{\frac{1}{2-\alpha}} = V_{0\alpha}(\eta_0/\eta_1)^{\frac{1}{2-\alpha}}$, and the rim width is enlarged: $\Delta_{1\alpha} = ((\frac{2-\alpha}{2})V_1^\alpha/v_\alpha^\alpha)^{\frac{1}{2-\alpha}}\Delta_1 = \Delta_{0\alpha}(\eta_1/\eta_0)^{\frac{1-\alpha}{2-\alpha}}$.
- Between τ_0 and τ_1 the elasticity prevent the height of the rim from increasing, and the increase of the rim width $W \sim L$ leads to a rapid decrease of the dewetting velocity:

$$V(t) \simeq V_{1\alpha}\left(\frac{t}{\tau_1}\right)^{-\frac{1}{2-\alpha}} \qquad (22)$$

  in agreement with the numerical resolutions (see Fig. 9). This result can be straightforwardly deduced from the simple scaling $V_{1\alpha}/V_{0\alpha} = (\tau_1/\tau_0)^{\frac{1}{2-\alpha}}$, or using the effective viscosity $\eta_{eff} = Gt$ in equation (19).

The decrease of the velocity is sharpened by the non-linearity of the friction. We notice that the decreasing law is close to t^{-1} if the exponent α is around one, as measured in the friction experiments cited above. The very weak variation of the friction force with the sliding velocity can thus explain the rapid decrease ($V \sim t^{-1}$) observed experimentally [22,23,25].

Among the experimental observations, a mystery still remains: the increase of the rim width proportionally to the dewetted distance is followed by a decrease of W [22, 23,25]. In the model proposed above, the rim width always increases, especially during the elastic regime. This increase is weaker when the friction is non-linear though: $W(t) \simeq \Delta_{1\alpha}(t/\tau_1)^{\frac{1-\alpha}{2-\alpha}}$ (it even becomes logarithmic when α tends toward unity). However, the rim width is now a function of the amplitude of the dewetting driving forces (*i.e.* the capillary forces in usual cases: $\Delta_{1\alpha} \sim |S|^{\frac{\alpha}{2-\alpha}}$). A decrease of the rim width can thus be expected if the driving forces decrease during the dewetting process.

A variation of the driving force with time would also explain the important variations of the initial dewetting velocity observed when varying the aging time. Such driving force could be the residual stresses resulting from the spin coating process. In the following section, we study the consequences of the presence of residual stresses which could relax during the aging below T_g over a characteristic time of the order of years. Above T_g, the characteristic relaxation time is τ_1.

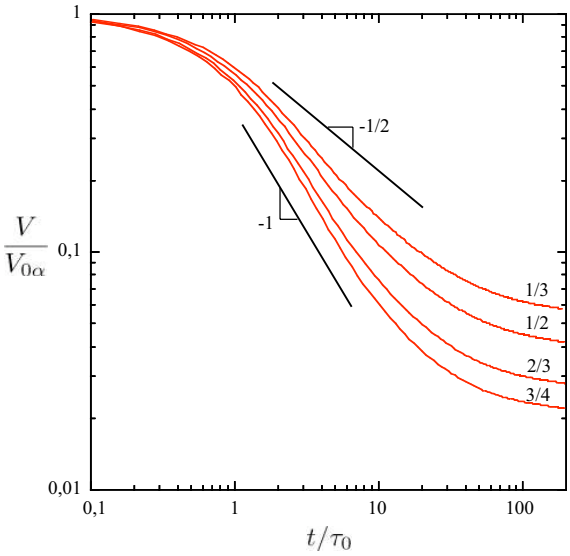

Fig. 9. Numerical calculations of the reduced dewetting velocities $V/V_{0\alpha}$ *versus* the reduced time t/τ_0 for a viscoelastic film ($\tau_1 = 100\,\tau_0$, $h_0G/|S| = 10$) dewetting on several substrates with the friction exponents $\alpha = 1/3$, $1/2$, $2/3$, and $3/4$.

5 Aging and residual stresses

5.1 Residual stresses

Systematic experimental studies have shown that the initial dewetting velocity decreases if the sample is held below T_g for a given amount of time [25,26]. We will see in this subsection that this variation of the initial dewetting velocity with the aging time can be attributed to a variation of residual stresses present within the film at the very beginning of the dewetting process. We first focus on the dewetting with a linear-friction force.

Elastic stresses relax in a static viscoelastic liquid over the characteristic time τ_1. If present at the beginning of the dewetting process, they will modify the dynamic during the first two regimes ($t < \tau_1$), but not during the long-time Newtonian regime ($t > \tau_1$). Thus, if the residual stresses increase the initial dewetting velocity, they will also give a more rapid decrease of the velocity down to the final velocity V_1.

We consider a film with the frozen homogeneous positive horizontal stress σ_0 at $t < 0$. The power delivered by the residual stresses is given by $\int h(x,t)\sigma(x,t)\dot{\gamma}(x,t)\mathrm{d}x$, which is simply equal to $h_0\sigma_0 V_i$, at $t = 0^+$, where V_i is the initial dewetting velocity. Additionally, this stress modifies the evolution of the height of the rim with time.

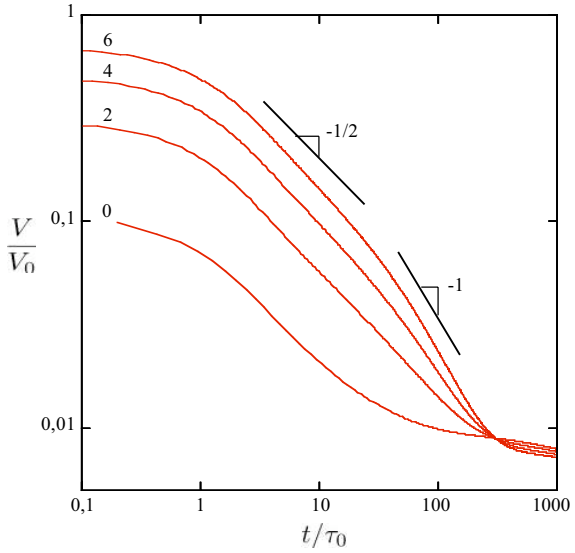

Fig. 10. Numerical calculations of the reduced dewetting velocities V/V_0 *versus* the reduced time t/τ_0 for a viscoelastic film ($\tau_1 = 100\,\tau_0$, $h_0 G/|S| = 10$) with the residual stresses $\sigma_0/G = 0$, 0.2, 0.4, and 0.6, dewetting on a substrate with a linear friction.

Equation (13) still holds, but the initial conditions are different. Then, the initial growth rate of the height $H(t)$ is $|S|/\eta_0 + \sigma_0 h_0/\eta_0$. Now, adding the power $h_0\sigma_0 V_i$ to the left-hand side of equation (11) with the initial increasing rate of $H(t)$ calculated above, we obtain the initial dewetting velocity

$$V_i = V_0 \left(1 + \frac{\sigma_0 h_0}{|S|}\right). \tag{23}$$

As expected, the residual stresses are responsible for a higher initial dewetting velocity. They are in fact equivalent to an additional capillary force $\sigma_0 h_0$ by unit of length. As the increasing rates of $H(t)$ and $L(t)$ are enhanced similarly, the rim width is not modified by the presence of residual stresses: $W \simeq \Delta_0$ until τ_0. This is due to the fact that Δ_0 does not depend on the dewetting driving force $|S|$ if the friction is linear, contrary to V_0 which linearly depends on it.

Around τ_0 the elasticity imposes a slowing-down of the increase of $H(t)$, down to the rate $|S|/\eta_1$. Between τ_0 and τ_1 the height of the rim is approximately constant, $H(t) \simeq h_0 + |S|(1 + h_0\sigma_0/|S|)/G$, and the residual stresses have not relaxed much yet. Hence, equation (11) with the additional contribution of the residual stresses still gives a decrease of the dewetting velocity proportional to $t^{-1/2}$. The stressed film is thus perfectly equivalent to a relaxed film pushed by the force $|S| + h_0\sigma_0$ by unit of length until the time τ_1. The decrease is more rapid only around the time τ_1 as the residual stresses relax within the film [31]. At longer times than τ_1, we recover the dewetting velocity V_1 and rim width Δ_1. These results agree with the numerical resolution of the problem (see Fig. 10).

Finally, for positive residual stresses lead to an enhancement of the dewetting velocity, their presence could suitably explain a decrease of the initial dewetting velocity with the aging time. We note that when using a linear-friction force, the evolution of the rim width with time is not qualitatively modified by the residual stresses: W still increases from Δ_0 to Δ_1 during the elastic regime, and then levels off. The non-linear friction could explain the existence of a maximum of the rim width, whose amplitude decreases with the aging time, for it leads to a dependence of the rim width on the dewetting velocity.

5.2 Residual stresses plus non-linear friction: the winning duo

We now combine the non-linear friction and residual stresses. We have shown in the previous subsection that the residual stresses are equivalent to an additional capillary force $\sigma_0 h_0$ until the time τ_1. Therefore, using the results of the previous section concerning the dewetting with a non-linear–friction force, the initial dewetting velocity simply reads

$$V_i = V_{0\alpha} \left(1 + \frac{h_0\sigma_0}{|S|}\right)^{\frac{2}{2-\alpha}}. \tag{24}$$

In the same way, the initial rim width, which depends on the capillary forces when the friction is non-linear, is increased by the presence of residual stresses: $\Delta_i = \Delta_{0\alpha}(1 + h_0\sigma_0/|S|)^{\frac{\alpha}{2-\alpha}}$. Then, from τ_0 to τ_1, the dewetting velocity decreases with time as $V(t) \simeq V_i(t/\tau_1)^{-\frac{1}{2-\alpha}}$, while the rim width increases up to its maximum value:

$$\Delta_m \simeq \Delta_{1\alpha} \left(1 + \frac{h_0\sigma_0}{|S|}\right)^{\frac{\alpha}{2-\alpha}}. \tag{25}$$

This is indeed the maximum of the rim width in time, as the relaxation of the residual stresses around τ_1 leads to a decrease of the dewetting velocity down to the "equilibrated" velocity $V_{1\alpha}$, as well as to a slow decrease of the rim width down to its "equilibrated" value $\Delta_{1\alpha}$. At this point, the decrease of $W(t)$ is as slow as the increase of $L(t)$, for only the front of the rim is moving. Then, when $t \gg \tau_1$, one recovers the long-times Newtonian-like dewetting. The decrease of the rim width can thus be explained by the combined consequences of the residual stresses and the non-linearity of the friction law. As a matter of fact, Δ_m is higher than $\Delta_{1\alpha}$ only if the exponent α and σ_0 are not nil. This striking result is also obtained with the numeric resolutions of the flow equations (see Figs. 11 and 12).

Interestingly, the residual stresses σ_0 can come off from the relation between the initial dewetting velocity V_i and the maximum rim width Δ_m:

$$V_i = v_\alpha \left(\frac{\zeta}{h_0}\right)^{\frac{1}{\alpha}} \eta_0^{-\frac{1}{2-\alpha}} \eta_1^{-\frac{2(1-\alpha)}{2-\alpha}} \Delta_m^{\frac{2}{\alpha}}. \tag{26}$$

The exponent α can thus be deduced from a log-log plot of V_i as a function of Δ_m, for dewetting experiments with various values of the residual stress. Furthermore, there

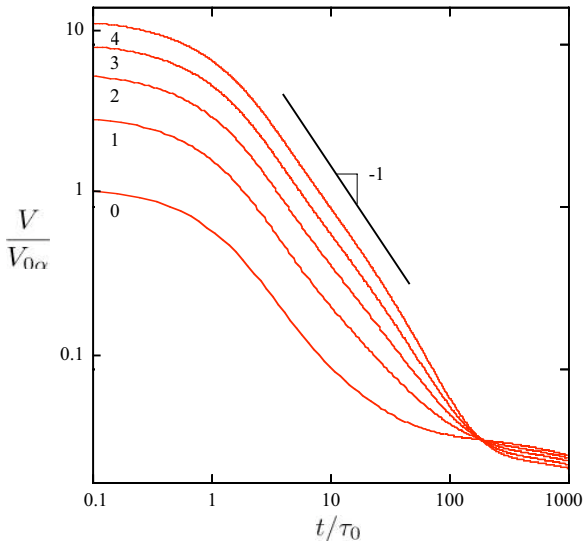

Fig. 11. Numerical calculations of the reduced dewetting velocities $V/V_{0\alpha}$ *versus* the reduced time t/τ_0 for a viscoelastic film ($\tau_1 = 100\,\tau_0$, $h_0G/|S| = 5$) with the residual stresses $\sigma_0/G = 0$, 0.2, 0.4, 0.6, and 0.8, dewetting on a substrate with the friction exponents $\alpha = 2/3$.

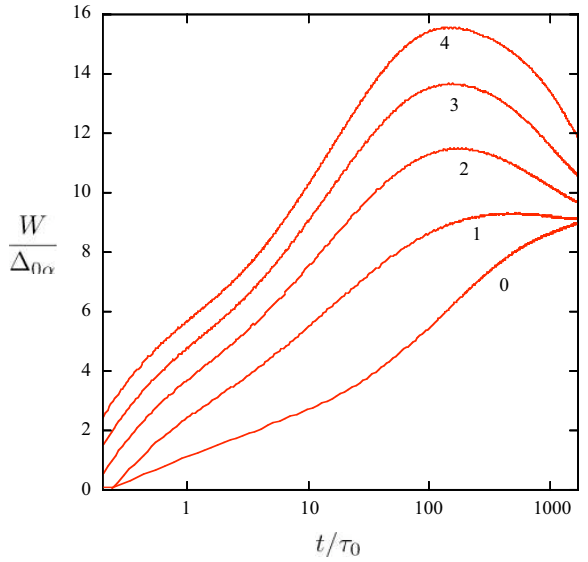

Fig. 12. Numerical calculations of the reduced rim width $W/\Delta_{0\alpha}$ *versus* the reduced time t/τ_0 for a viscoelastic film ($\tau_1 = 100\,\tau_0$, $h_0G/|S| = 5$) with the residual stresses $\sigma_0/G = 0$, 0.2, 0.4, 0.6, and 0.8, dewetting on a substrate with the friction exponents $\alpha = 2/3$.

is a weak dependence of $V_i/\Delta_m^{\frac{2}{\alpha}}$ on the viscosity η_1, and thus on the molecular weight of the polymer, when α is close to unity. Then, log-log plots corresponding to different molecular weights can be superposed in order to measure α. This has been done in [26], giving a friction exponent $\alpha = 0.8 \pm 0.15$. This value is very close to the values presented above for the friction between a PDMS elastomer and a grafted brush [7], although almost no interpenetration is expected between the PS film and the PDMS layer. The non-linear relation between friction and velocity could thus be a consequence of the rheologic response of the brush to a shear strain only, *i.e.* shear thinning, and not to a variation of the interdigitation with the sliding velocity [32].

Once the friction exponent α is determined, a quantitative evaluation of the residual stresses becomes possible. The quantities τ_1 (the time corresponding to the maximum rim width), $V_{1\alpha}$, and $\Delta_{1\alpha}$ can directly be deduced from the plots of $W(t)$ and $L(t)$. From these measures we can calculate the ratio $h_0G/|S| = \Delta_{1\alpha}/(\tau_1 V_{1\alpha})$. Then σ_0 is simply deduced from the measurement of Δ_m. It shows that σ_0 can be as large as G [26], in agreement with [28], which is significant. Note that since the time τ_0 cannot be accurately evaluated, one cannot obtain a precise evaluation of ζ and v_α.

It has been noticed that the characteristic relaxation time of elastic constraints τ_1 is significantly shorter than the corresponding relaxation time in bulk (*i.e.* the reptation time of the polymer chains) [25,26], which is consistent with the fact that the entanglement length should be longer in films whose thickness is of the order of the molecules size [36,37]. Still, the question of the structure of the chains in a spin-coated film is nowadays unanswered. Are they very stretched and weakly entangled, or structured in isolated balls with small interpenetration?

Finally, the idea of a non-linear friction proves its pertinence by the fact that the exponent α deduced from the relation between Δ_m and V_i, gives the good scaling law ($V \sim t^{-0.8}$) for the decrease of the dewetting velocity.

6 The case of circular holes

When the dewetting process is not initiated from an edge, but from a circular hole, BW showed that the dynamic is first dominated by viscous dissipation within the radial flow, and that the consequences of the friction on the substrate are negligible [4]. The growth of the hole is then exponential in time for a Newtonian liquid. Now that the viscoelasticity has been shown to be an important physical property concerning the dewetting from a straight edge, it is of interest to study the role it plays during the early part of the dewetting from a hole (*i.e.* neglecting the friction on the substrate). At the same time, the consequences of residual stresses should be addressed.

In this two-dimension problem, the cylindrical coordinates should be used, giving constitutive equations similar to equation (12):

$$\begin{aligned} \sigma_r - \nu\sigma_\theta + \tau_1(\dot{\sigma_r} - \nu\dot{\sigma_\theta}) &= \eta_1\left(\dot{\gamma_r} + \tau_0(\ddot{\gamma_r} - \nu\ddot{\gamma_\theta})\right), \\ \sigma_\theta - \nu\sigma_r + \tau_1(\dot{\sigma_\theta} - \nu\dot{\sigma_r}) &= \eta_1\left(\dot{\gamma_\theta} + \tau_0(\ddot{\gamma_\theta} - \nu\ddot{\gamma_r})\right), \end{aligned} \quad (27)$$

in the radial and the orthoradial directions, with $\tau_0 = \eta_0/G$, $\tau_1 = \eta_1/G$ ($\tau_0 \ll \tau_1$), and ν is Poisson's ratio. This Jeffreys' model can be approximated by a Voigt's model at short times (for $t \ll \tau_1$, $\sigma \ll \tau_1\dot{\sigma}$), which means that the relaxation of the elastic stress due to the disentanglements of the polymer chains is negligible. At long times it can be approximated by a pure Maxwell's model (for $t \gg \tau_0$,

$\dot{\gamma} \gg \tau_0 \ddot{\gamma}$), as the dissipation due to the monomers viscosity η_0 is negligible compared to the dissipation due to the disentanglements of the polymer chains η_1. The opening of holes in a viscoelastic film can then be divided into two parts that overlap: $t \ll \tau_1$ and $t \gg \tau_0$.

6.1 Early opening: Voigt's model

In this regime, as no relaxation of the stress is allowed, the elastic stress corresponding to the elastic modulus G, and the viscous stress corresponding to the viscosity η_0 are simply superposed:

$$\begin{aligned} \dot{\sigma_r} - \nu\dot{\sigma_\theta} &= G\left(\dot{\gamma_r} + \tau_0(\ddot{\gamma_r} - \nu\ddot{\gamma_\theta})\right), \\ \dot{\sigma_\theta} - \nu\dot{\sigma_r} &= G\left(\dot{\gamma_\theta} + \tau_0(\ddot{\gamma_\theta} - \nu\ddot{\gamma_r})\right). \end{aligned} \tag{28}$$

We can first consider the opening of a hole of initial radius R_0 in a purely elastic film initially homogeneously constrained with the stress σ_0. Applying a pressure p at the edge, in the small deformation approximation the film stays uniformly flat, with the thickness h_0, giving the repartition of stress [38],

$$\begin{aligned} \sigma_r(r) &= \sigma_0 - (\sigma_0 + p)\frac{R^2}{r^2}, \\ \sigma_\theta(r) &= \sigma_0 + (\sigma_0 + p)\frac{R^2}{r^2}, \end{aligned} \tag{29}$$

for $r \geqslant R$, and the hole radius $R = R_0 \exp((1+\nu)(\sigma_0 + p)/G)$.

Considering a purely Newtonian film of viscosity η_0, the repartition of stress corresponding to the velocity field $v(r) = \dot{R}R/r$ (constant thickness) is

$$\begin{aligned} \sigma_r(r) &= -\eta_0 \frac{R\dot{R}}{r^2}, \\ \sigma_\theta(r) &= \eta_0 \frac{R\dot{R}}{r^2}. \end{aligned} \tag{30}$$

The sum of these two contributions, elastic and viscous, with the boundary condition $\sigma_r(R) = -|S|/h_0$, and the relation $p(R) = -\sigma_0 + G\ln(R/R_0)/(1+\nu)$ leads to the dynamic equation

$$\frac{\dot{R}}{R} + \frac{G}{(1+\nu)\eta_0}\ln\left(\frac{R}{R_0}\right) = \frac{|S|}{\eta_0 h_0} + \frac{\sigma_0}{\eta_0} \tag{31}$$

whose solution reads

$$R(t) = R_0 \exp\left[\frac{(1+\nu)|S|}{h_0 G}\left(1 + \frac{\sigma_0 h_0}{|S|}\right)\left(1 - e^{\frac{-t}{(1+\nu)\tau_0}}\right)\right]. \tag{32}$$

Hence, the initial opening law is exponential until the hole radius reaches $R_0^* = R_0 \exp((1+\nu)(|S|/h_0 G)(1 + \sigma_0 h_0/|S|))$ around the time $(1+\nu)\tau_0$. Then, the hole radius does not change until the stress relaxes ($t \sim \tau_1$). This result can also be obtained from the energy balance between the power $2\pi|S|R\dot{R}$ released by the capillary forces, and the sum of the viscous dissipation $-2\pi\eta_0 h_0 \dot{R}^2$ and the variation of the elastic energy $2\pi p(R) R\dot{R}$. We note that, unlike in the edge geometry, a purely elastic film would not dewet more than over the distance R_0^*.

During this regime, while $\sigma_r(R)$ is constant in time, $\sigma_\theta(R)$ increases linearly up to $\sigma_{max} \simeq 2\sigma_0 + |S|/h_0$ at time $(1+\nu)\tau_0$, which is more than twice its initial value σ_0. Hence, this opening could lead to the appearance of cracks normal to the edge of the hole, if σ_{max} is larger than the rupture threshold of the polymer chains. Such cracks have indeed been observed by Damman *et al.* [39].

6.2 Second step: Maxwell's model

At times larger than τ_0, the dissipation due to the monomers viscosity η_0 is weak compared to the dissipation due to the relaxation of the elastic stress, which can be associated to a viscosity $\eta_1 \ll \eta_0$:

$$\begin{aligned} \sigma_r - \nu\sigma_\theta + \tau_1(\dot{\sigma_r} - \nu\dot{\sigma_\theta}) &= \eta_1\dot{\gamma_r}, \\ \sigma_\theta - \nu\sigma_r + \tau_1(\dot{\sigma_\theta} - \nu\dot{\sigma_r}) &= \eta_1\dot{\gamma_\theta}. \end{aligned} \tag{33}$$

In this Maxwell's model, the relaxation of the stress over the characteristic time τ_1 gives a viscous dissipation by volume unit equal to $-(\sigma_r(\sigma_r - \nu\sigma_\theta) + \sigma_\theta(\sigma_\theta - \nu\sigma_r))/\eta_1$, which is the elastic energy u_{el} divided by $\tau_1/2$. The variation of the elastic energy by volume unit with time is simply $\dot{u_{el}} = (\sigma_r(\dot{\sigma_r} - \nu\dot{\sigma_\theta}) + \sigma_\theta(\dot{\sigma_\theta} - \nu\dot{\sigma_r}))/G$. Finally, the sum of the two, $\sigma_r\dot{\gamma_r} + \sigma_\theta\dot{\gamma_\theta}$, is the power delivered to the material. The conservation of the energy imposes the equality between the integral of this quantity over all the volume of the material and the power released by the capillary forces:

$$2\pi|S|R\dot{R} = 2\pi h_0 \int_R^\infty (\sigma_r\dot{\gamma_r} + \sigma_\theta\dot{\gamma_\theta}) r\mathrm{d}r. \tag{34}$$

Assuming the film to stay flat during its opening, the stress distribution is simply

$$\begin{aligned} \sigma_r(r) &= \sigma_\infty - \left(\sigma_\infty + \frac{|S|}{h_0}\right)\frac{R^2}{r^2}, \\ \sigma_\theta(r) &= \sigma_\infty + \left(\sigma_\infty + \frac{|S|}{h_0}\right)\frac{R^2}{r^2}, \end{aligned} \tag{35}$$

where $\sigma_\infty = \sigma_0 \exp(-t/\tau_1)$ is the relaxing stress, infinitely far from the edge of the hole. Using relations (33), and (35) in equation (34) leads to the result [40]

$$\frac{\dot{R}}{R} = \frac{1+\nu}{\tau_1}\left(\frac{|S|}{h_0 G} + \frac{\sigma_\infty(t)}{G}\right) \tag{36}$$

in the small deformation limit corresponding to $|S|/h_0 \ll G$, and $\sigma_\infty/G \ll \sqrt{|S|/h_0 G}$. Out of these limits the film no longer stays flat. Then, in the small deformation limit, the opening of the hole is quasi-exponential:

$$R(t) = R_0^* \exp\left[(1+\nu)\left(\frac{|S|}{h_0 G}\frac{t}{\tau_1} + \frac{\sigma_0}{G}\left(1 - e^{-\frac{t}{\tau_1}}\right)\right)\right]. \tag{37}$$

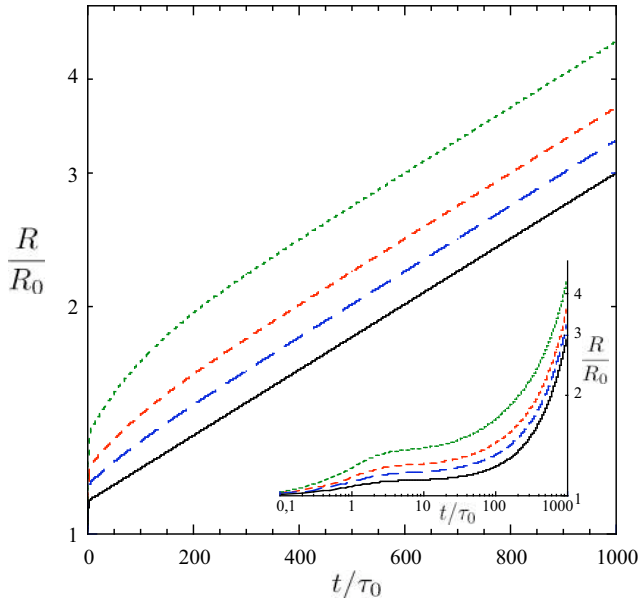

Fig. 13. Time evolution of the radius R/R_0 of a hole opening in a free-standing viscoelastic film ($\tau_1 = 100\,\tau_0$, $h_0G/|S| = 10$), with the residual stresses $\sigma_0 h_0/|S| = 0$ (plain line), 1/2, 1, and 2 (dotted line).

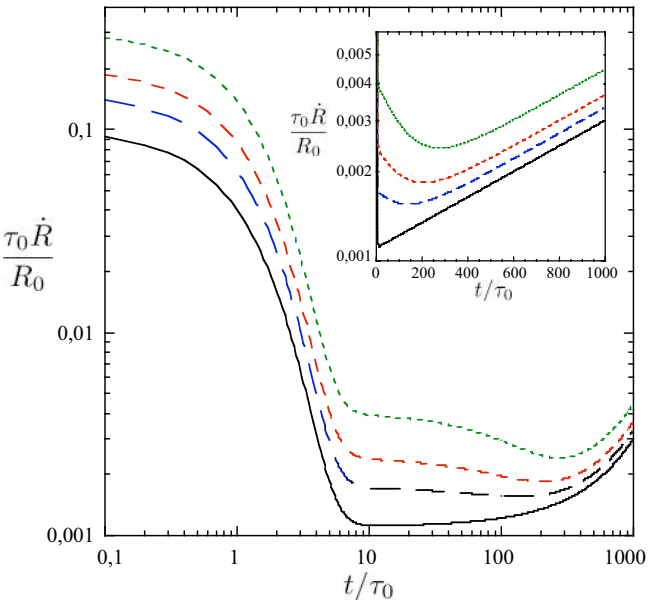

Fig. 14. Time evolution of the opening velocity $\tau_0\dot{R}/R_0$ of a hole in a free-standing viscoelastic film ($\tau_1 = 100\,\tau_0$, $h_0G/|S| = 10$), with the residual stresses $\sigma_0 h_0/|S| = 0$ (plain line), 1/2, 1, and 2 (dotted line).

As the solution equation (32) we obtained for the first regime is approximately constant after the time τ_0, and as the above solution equation (37) in the second regime very weakly varies before τ_0, we can build an approximated solution valid at all times replacing R_0^* in equation (37) by the solution equation (32) (see Figs. 13 and 14).

Finally we note that, as in the edge geometry, the initial dewetting velocity is high and independent of η_1 ($\dot{R} \sim R_0/\tau_0$). On the other hand, the viscoelasticity leads, in the hole geometry, to a sudden fall of the dewetting velocity around τ_0. The velocity hence reaches a low value, which depends on η_1 ($\dot{R} \sim R_0/\tau_1$), at the very short time $(1+\nu)\tau_0 \ln(\tau_1/\tau_0) \sim \tau_0$, while it progressively decreases between τ_0 and τ_1 in the edge geometry. For the time τ_0 is typically not accessible to the experimentalists, the initial high dewetting velocity should not be observed in the hole geometry. This is in agreement with the observations of Reiter, Damman *et al.* [22,23] where the observed initial dewetting velocity is systematically orders of magnitude higher in the edge geometry than in the hole geometry.

Furthermore, this model predicts a very slow increase of the opening velocity, with the characteristic rising time $(|S|/h_0G)\tau_1 < \tau_1$, between τ_0 and τ_1, while the velocity rapidly decreases between τ_0 and τ_1 in the edge geometry. This explains the other observation of an almost constant opening velocity of the holes, while in the meantime the dewetting velocity at the edge of the film decrease of several orders of magnitudes with a t^{-1} law [22,23]. The variation of the dewetting velocity is even weaker in the presence of residual stress; the weak increase is replaced by a weak decrease of the velocity between τ_0 and τ_1, if $\sigma_0 > |S|/h_0$ (see Fig. 14). As we could have anticipated, the opening is accelerated by the residual stress until the time τ_1 where the stress relaxes, and then the velocity recovers an exponential growth. This characteristic behavior (see Fig. 13) is what Roth *et al.* [16] observe during the opening of holes in free-standing PS films of large molecular weights close to the glass transition. The high similarity between their experimental plots and the theoretical curves of Figure 13 leads to the conclusion that their PS films also present residual stresses. Actually, these films, formed by spin coating, are not annealed above the glass transition.

Eventually, as for Newtonian films, the friction on the substrate will become dominant when the hole radius R is larger than the distance $\Delta_{1\alpha}$ (this corresponds to $t > \tau_1(h_0G/|S|)\ln(\Delta_{1\alpha}/R_0^*)$). Then the dewetting from holes becomes comparable to the dewetting from edges.

7 Conclusion

In this paper we have reviewed some important features of the dewetting of slipping polymer films. One of the most important properties of entangled polymer liquids is viscoelasticity, whose basic characteristics can by captured by a Maxwell's model, with the elastic modulus G and the relaxation time τ_1. One of the consequences of the viscoelasticity on the dewetting of the film from a straight edge is a slowing-down of the dewetting velocity over the time τ_1. The scaling of this decreasing law depends on the friction between the film and the substrate. A consequence of the friction is the formation of a rim, which stays very asymmetric until a characteristic time which is typically larger than τ_1. The time evolution of the rim width together with the dewetted distance, which is easy to follow experimentally, give important information about the friction and about the elasticity of the film. Viscoelastic

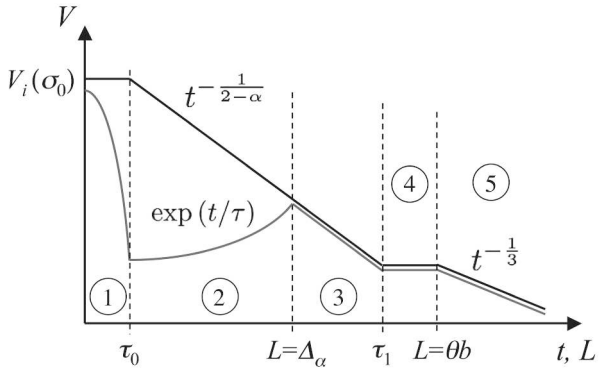

Fig. 15. Schematic representation of the different dewetting dynamic regimes in both the straight-edge (black line) and the hole geometry (gray line): (1) Short-time dewetting, (2) elastic regime with negligible influence of the friction in the hole geometry, (3) elastic regime with strong influence of the friction in both geometries, (4) Newtonian asymmetric-rim regime, (5) mature-rim regime.

films can contain internal residual stress if stored below the glass transition temperature. These residual stresses accelerate the onset of the dewetting process, and leave a signature on the time evolution of the rim width, which allows a quantitative evaluation. The signature of the viscoelasticity and the residual stresses are also visible when the dewetting is initiated from a hole, giving a very fast first opening stage, followed by a slow, quasi-exponential, growth of the hole radius. A schematic representation of the dewetting dynamic in both the straight-edge and the hole geometry is shown on Figure 15. We can infer that, as the residual stresses increase the first opening stage velocity of holes, the residual stresses can initiate the formation of holes from thickness defects [41], which could explain the decrease of the holes number density with the aging time of the PS samples also observed in [25].

We gratefully thank Günter Reiter and Pascal Damman for very fruitful discussions and extensive collaboration. We also thank Pierre-Gilles de Gennes for useful comments.

References

1. P.-G. de Gennes, F. Brochard-Wyart, D. Quéré, *Capillarity and Wetting Phenomena: Drops, Bubbles, Pearls, Waves* (Springer, 2003).
2. P.-G. de Gennes, C. R. Acad. Sci. B **288**, 219 (1979).
3. C. Redon, J.B. Brzoska, F. Brochard-Wyart, Macromolecules **27**, 468 (1994).
4. F. Brochard-Wyart, G. Debrégeas, R. Fondecave, P. Martin, Macromolecules **30**, 1211 (1997).
5. R.B. Bird, R.C. Armstrong, O. Hassager, *Dynamics of Polymeric Liquids*, Vol. **1** (John Wiley & Sons, 1977).
6. A. Casoli, M. Brendlé, J. Schultz, P. Auroy, G. Reiter, Langmuir **17**, 388 (2001).
7. L. Bureau, L. Léger, Langmuir **20**, 4523 (2004).
8. A. Oron, S.H. Davis, S.G. Bankoff, Rev. Mod. Phys. **69**, 931 (1997).
9. G. Reiter, J. Forrest, Eur. Phys. J. E **8**, 101 (2002).
10. P.F. Green, V. Ganesan, Eur. Phys. J. E **12**, 449 (2003).
11. D.G. Bucknall, Prog. Mater. Sci. **49**, 713 (2004).
12. R. Seemann, S. Herminghaus, K. Jacobs, Phys. Rev. Lett. **87**, 196101 (2001).
13. S. Herminghaus, R. Seemann, K. Jacobs, Phys. Rev. Lett. **89**, 056101 (2002).
14. R. Fetzer, K. Jacobs, A. Münch, B. Wagner, T.P. Witelski, Phys. Rev. Lett. **95**, 127801 (2005).
15. M. Rauscher, A. Münch, B. Wagner, R. Blossey, Eur. Phys. J. E **17**, 373 (2005).
16. C. Roth, B. Deh, B.G. Nickel, J.R. Dutcher, Phys. Rev. E **72**, 021802 (2005).
17. J.H. Xavier, M.H. Rafailovich, J. Sokolov, Langmuir **21**, 5069 (2005).
18. G. Reiter, R. Khanna, Langmuir **16**, 6351 (2000).
19. G. Reiter, Phys. Rev. Lett. **87**, 186101 (2001).
20. F. Saulnier, E. Raphaël, P.-G. de Gennes, Phys. Rev. Lett. **88**, 196101 (2002); Phys. Rev. E **66**, 061607 (2002).
21. V. Shenoy, A. Sharma, Phys. Rev. Lett. **88**, 236101 (2002).
22. P. Damman, N. Baudelet, G. Reiter, Phys. Rev. Lett. **91**, 216101 (2003).
23. G. Reiter, M. Sferrazza, P. Damman, Eur. Phys. J. E **12**, 12 (2003).
24. T. Vilmin, E. Raphaël, Europhys. Lett. **72**, 781 (2005).
25. G. Reiter, M. Hamieh, P. Damman, S. Sclavons, S. Gabriele, T. Vilmin, E. Raphaël, Nat. Mater. **4**, 754 (2005).
26. T. Vilmin, E. Raphaël, G. Reiter, M. Hamieh, P. Damman, S. Sclavons, S. Gabriele, Europhys. Lett. **73**, 906 (2006).
27. G. Reiter, P.-G. de Gennes, Eur. Phys. J. E. **6**, 25 (2001).
28. H. Bodiguel, C. Fretigny, Eur. Phys. J. E **19**, 185 (2006).
29. P.-G. de Gennes, Langmuir **12**, 4497 (1996).
30. P.-G. de Gennes, private communication.
31. For $t > \tau_0$ the height of the rim is approximately $H(t) = h_0 + |S|(1 + h_0\sigma_0/|S| + t/\tau_1)/G$ (assuming $|S| + h_0\sigma_0 < h_0G$, otherwise $(H(\tau_0)/h_0)(\ln(H(\tau_0)/h_0) - \sigma_0/G) = |S|/(h_0G)$). As the residual stress is nil at the front of the film and relaxes far away from the rim ($\sigma(x \gg W) = \sigma_0 \exp(-\frac{t}{\tau_1})$), the power released by the residual stresses $h_0\sigma_0 \exp(-\frac{t}{\tau_1}) V(t)$ slowly decreases. Equation (11) with the additional contribution of the residual stresses now gives the dewetting velocity:

$$V(t) \simeq \frac{V_1}{\sqrt{2}} \frac{\left(1+\epsilon+\frac{t}{\tau_1}\right)\left(1+\epsilon e^{-\frac{t}{\tau_1}}\right)}{\sqrt{\frac{t}{\tau_1}+\frac{1}{2}\left(\frac{t}{\tau_1}\right)^2+\epsilon\left(2+\epsilon+\frac{t}{\tau_1}\right)\left(1-e^{-\frac{t}{\tau_1}}\right)}}$$

for times larger than τ_0 ($\epsilon = h_0\sigma_0/|S|$). Note that when the capillary forces are negligible (*i.e.* $\epsilon \gg 1$), the residual stresses alone are able to induce the dewetting process, and lead to a decrease of the dewetting velocity like $\exp(-t/\tau_1)$.
32. The theoretical explanation for the weak increase of the friction between an elastomer and a grafted layer has not yet been found, and it is not clear whether it is only due to a variation of the interdigitation or not. Indeed, polymer melts have a shear-thinning behavior at large enough shear rates [33,34]. Although the shear rate in the very thin PDMS layer is larger than in the film, it may not be large enough to explain the non-linearity of the friction in the large velocity range explored by Bureau *et al.* [7]. However, it has been shown that the shear rate above which shear

thinning is observed in melts is very weak if the polymer chains are branched and cannot reptate [35]. Therefore, the fact that the grafted chains cannot reptate could explain a very low velocity v_α.

33. M. Doi, S.F. Edwards, *The Theory of Polymer Dynamics* (Clarendon Press, Oxford, 1986).
34. D.W. Mead, R.G. Larson, M. Doi, Macromolecules **31**, 7895 (1998).
35. S.T. Milner, T.C.B. McLeish, Macromolecules **30**, 2159 (1997).
36. M.K. Sanyal, J.K. Basu, A. Datta, S. Banerjee, Europhys. Lett. **36**, 265 (1996).
37. L. Si, M.V. Massa, K. Dalnoki-Veress, H.R. Brown, R.A.L. Jones, Phys. Rev. Lett. **94**, 127801 (2005).
38. S.P. Timoshenko, J.N. Goodier, *Theory of Elasticity* (McGraw-Hill International Editions, 1970).
39. P. Damman, private communication.
40. The complete relation is

$$\frac{\dot{R}}{R} = \frac{1+\nu}{\tau_1} \frac{\frac{|S|}{h_0 G} + \frac{\sigma_\infty}{G}}{1 - (1+\nu)\frac{h_0 G}{|S|}\left(\frac{|S|}{h_0 G} + \frac{\sigma_\infty}{G}\right)^2}.$$

We note that $\dot{R}/R$ diverges if $|S|/h_0 = G/(1+\nu)$, or $\sigma_\infty/G = \sqrt{|S|/((1+\nu)h_0 G)}$, which is due to the fact that the film cannot stay flat any more. Interestingly, if there are no capillary forces, $|S| = 0$, the hole radius stays constant, whatever the value of the residual stress σ_∞. On the other hand, if one adds a weak capillary force $|S|/h_0 G < (1+\nu)(\sigma_\infty/G)^2$, their is no solution to the energy balance because the assumption that the film stays flat does not hold any more.

41. T. Vilmin, E. Raphaël, Phys. Rev. Lett. **97**, 036105 (2006).